12-1-2015

Ecohydrological Controls on Grass and Shrub Above-ground Net Primary Productivity in a Seasonally Dry Climate

Anthony J. Parolari
Marquette University, anthony.parolari@marquette.edu

Michael L. Goulden
University of California, Irvine

Rafael L. Bras
Georgia Institute of Technology

Accepted version *Ecohydrology,* Vol. 8, No. 8 (December 2015): 1572-1583. DOI.

Ecohydrology, Vol. 8**,** No. 8 (February 2015): 1572-1583. DOI.

Ecohydrological controls on grass and shrub above-ground net primary productivity in a seasonally dry climate

Anthony J. Parolari
Department of Civil, Construction, and Environmental Engineering, Marquette University, Milwaukee, WI, USA
Nicholas School of the Environment, Duke University, Durham, NC, USA
Department of Civil and Environmental Engineering, Massachusetts Institute of Technology, Cambridge, MA, USA

Michael L. Goulden
Department of Earth System Science, University of California, Irvine, CA, USA

Rafael L. Bras
School of Civil and Environmental Engineering, Georgia Institute of Technology, Atlanta, GA, USA
School of Earth and Atmospheric Sciences, Georgia Institute of Technology, Atlanta, GA, USA

Abstract

Seasonally dry, water-limited regions are often co-dominated by distinct herbaceous and woody plant communities with contrasting ecohydrological properties. We investigated the shape of the above-ground net

primary productivity (ANPP) response to annual precipitation (Pa) for adjacent grassland and shrubland ecosystems in Southern California, with the goal of understanding the role of these ecohydrological properties on ecosystem function. Our synthesis of observations and modelling demonstrates grassland and shrubland exhibit distinct ANPP-P_a responses that correspond with characteristics of the long-term P_a distribution and mean water balance fluxes. For annual grassland, no ANPP occurs below a 'precipitation compensation point,' where bare soil evaporation dominates the water balance, and ANPP saturates above the P_a where deep percolation and runoff contribute to the modelled water balance. For shrubs, ANPP increases at a lower and relatively constant rate across the P_a gradient, while deep percolation and runoff account for a smaller fraction of the modelled water balance. We identify precipitation seasonality, root depth, and water stress sensitivity as the main ecosystem properties controlling these responses. Observed ANPP-P_a responses correspond to notably different patterns of rain-use efficiency (RUE). Grass RUE exceeds shrub RUE over a wide range of typical P_a values, whereas grasses and shrubs achieve a similar RUE in particularly dry or wet years. Inter-annual precipitation variability, and the concomitant effect on ANPP, plays a critical role in maintaining the balance of grass and shrub cover and ecosystem-scale productivity across this landscape.

Keywords

soil moisture dynamics; seasonal climates; primary production; rain-use efficiency

Introduction

Semi-arid ecosystems are often characterized by a patchwork of plant communities, such as the herbaceous and woody vegetation mosaic found in regions with seasonally dry climate. Because of their socio-economic importance and vulnerability to change under future climate and land use conditions (Schlesinger et al., [43] ; Rietkerk et al., [37] ; Reynolds et al., [36] ; Schneider et al., [44]), a mechanistic understanding of the structure and function of such water-limited ecosystems is essential to their proper management. Extensive research has highlighted both bottom-up (i.e. competition for soil moisture and nutrients) and top-down (i.e. fire and herbivory) controls on the productivity of semi-arid woody and herbaceous vegetation (Scholes and Archer, [45]).

The link between primary productivity and precipitation is an important indicator of dryland function. At the scale of an individual site, the response of above-ground net primary productivity (ANPP) to annual precipitation (P_a) varies substantially with soil type, plant functional type (PFT) and climate. ANPP generally increases with P_a, with evidence for both linear (Briggs and Knapp, [3] ; Huxman et al., [20] ; Hsu et al., [19]) and nonlinear (saturating) (Hsu et al., [14]) ANPP-P_a responses. However, ANPP-P_a correlations are often weak, and in some cases, ANPP is insensitive to P_a (Sala et al., [40]).

Previous analyses of the ANPP-P_a relation have been relatively descriptive, and the ecohydrological basis for these patterns has yet to be explored in detail. Because of nonlinearity in the surface hydrological response to precipitation, interaction between the soil water balance and vegetation productivity may be one factor that controls the shape of the ANPP-P_a response. Annual evapotranspiration, the water flux that facilitates productivity, tends to saturate with increasing annual precipitation (Budyko, [4]). In addition, root depth places a fundamental constraint on soil water availability. Shallow root profiles are associated with increased non-productive water fluxes, runoff and leakage and decreased water storage volume (Sala et al., [39] ; Laio et al., [28]). Lastly, asynchronous precipitation and energy availability in seasonally dry climates may limit ecosystem water availability. In these ecosystems, a large fraction of precipitation occurs before the growing season and is susceptible to non-productive evaporation and leakage losses before roots can effectively compete for available soil moisture. Therefore, soil, climate and vegetation factors that affect the soil water balance response to precipitation may explain observed variability in ANPP-P_a patterns.

The link between P_a, soil moisture, and ANPP may also help explain the coexistence of woody and herbaceous vegetation under similar climate, soil, and disturbance regimes. To date, observations of ANPP-P_a responses

have been reported for a single PFT at a given site (e.g. Briggs and Knapp, [3]) or for multiple PFTs across sites (e.g. Sala et al., [39] ; Huxman et al., [20] ; Hsu et al., [19] ; Jin and Goulden, [25]). Modelling studies quantified soil water balance effects on ecological success and generally focused on simulated water stress, transpiration, or primary productivity as key indicators of vegetation patterns (Schwinning and Ehleringer, [47] ; van Wijk and Rodriguez-Iturbe, [55] ; Scanlon and Albertson, [41] ; Ivanov et al., [23] , [24] ; Viola et al., [50] ; Hwang et al., [21] ; del Jesus et al., [10] ; Feng et al., [14]). while water stress is difficult to validate, ANPP is a commonly measured ecological property that combines information on resource availability and competitive advantage. The integration of ANPP observations and ecohydrological models offers an opportunity to advance mechanistic understanding of how woody and herbaceous vegetation communities may coexist under similar environmental conditions.

This paper is focused on the ecohydrological mechanisms connecting ANPP and P_a in the seasonally dry, semi-arid climate of coastal Southern California. We address the following questions: How do ANPP-P_a patterns differ between adjacent grass and shrub communities that grow in the same soil and climate environment? Does interaction between precipitation, the soil water balance and productivity explain these observed ANPP-P_a patterns and their differences? And, finally, how do ANPP-P_a patterns inform understanding of grass–shrub coexistence in seasonally dry environments? Our analysis is based on results from multi-year rainfall manipulation experiments in two distinct communities, one dominated by annual grasses and the other by drought-deciduous shrubs. The two communities are immediately adjacent to each other, and historical aerial photographs demonstrate this pattern has been stable for at least 70 years. In addition to climate and disturbance history (i.e. fire), topographic and edaphic factors are consistent between these communities. First, we analyse the ANPP-P_a response for both PFTs, demonstrating distinct linear and nonlinear responses in the shrub and grass communities, respectively. Second, we apply a simple model coupling ANPP to soil moisture dynamics to investigate the role of ecohydrological processes in generating these ANPP-P_a patterns. Last, the observed ANPP-P_a patterns are used as a basis for understanding how inter-annual P_a variability facilitates the co-occurrence of grass and shrub communities at this site.

Loma Ridge Experiment

The Loma Ridge rainfall manipulation experiment was established in 2007 and is located in central Orange County, California (33.742°N, 117.704°W). The site consists of distinct annual grass (Bartolome et al., [2]) and drought-deciduous shrub communities (Rundel, [38]) (Figure [NaN]). Loma Ridge experiences a seasonal climate with, on average, 90% of annual rainfall occurring in the winter between November and April (Figure [NaN]). The local soil is homogeneous and characterized as sandy loam.

Experimental plots

Rainfall manipulation was conducted in the grass and shrub communities for 6 years (2007–2012) and 4 years (2009–2012), respectively. In each community, 24 rectangular plots are divided into eight replicates of three water input treatments: ambient, ambient minus 40% (dry), and ambient plus 40% (wet). Plot dimensions are 6.1 × 8.5 m (grass) and 12.2 × 18.3 m (shrub). Rainfall is excluded from dry plots with retractable clear polyethylene roofs that were closed during approximately half of the rain events (<5% of the days during a year). Water draining from the roofs was collected in polyethylene tanks for subsequent application to the wet plots using pressure compensated drip tubing. Excluded events and irrigation rates were chosen to simulate observed patterns in storm frequency and intensity. Roof operation and irrigation are identical for the grass and shrub plots. Ambient water input was measured half-hourly by tipping bucket.

Above-ground net primary productivity was measured at the end of each growing season. Grassland ANPP was determined in late April or May by harvesting two 14 × 50 cm strips in each plot. The samples were oven-dried at 60 °C for 4 days and subsequently weighed. Late season herbaceous growth (generally from May through July) accounted for less than 10% of ANPP and was not considered in our analysis.

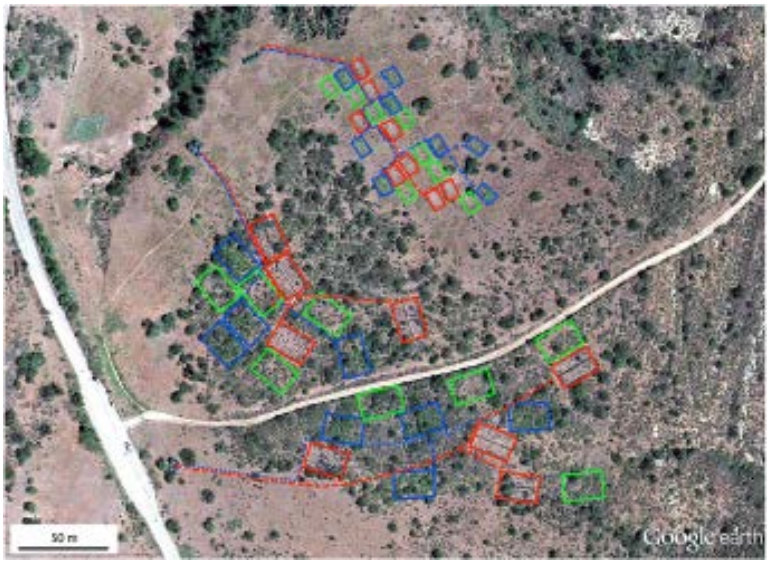

Figure 1. Loma Ridge study location indicating the location and orientation of adjacent grass (brown) and shrub (green) communities. The small rectangles outline the grass plots and the large rectangles outline the shrub plots (red = dry; green = ambient; blue = wet).

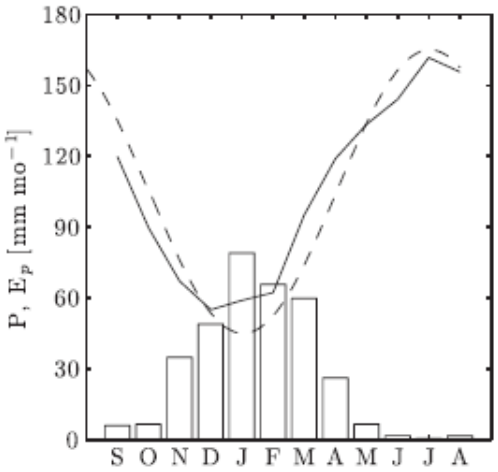

Figure 2. Loma Ridge seasonal cycle of precipitation (bars) and potential evapotranspiration (solid line). The dashed line indicates the sinusoidal approximation (Equation (13)).

Shrub ANPP was determined from direct measurements of the annual crown volume increase of the four most common species: Artemisia californica (ARCA), Malosma laurina (MALA), Salvia mellifera (SAME) and Acmispon glaber (ACGL). Averages of 6 ARCA, 9 MALA and 19 SAME shrubs were identified and permanently tagged in each shrub plot in October 2008 (a total of 807 plants). The volume of each shrub was recorded at the end of each growing season of each year (during August to October) using a ruler to measure the plant's width (w), depth (d) and height (h). Plant volume was calculated as the product of the measurements [i.e. v = wdh (cm^3)] and converted to mass (m), using allometric equations determined by harvest at the site (ARCA: $m = 0.0002v + 37.6$, $r^2 = 0.8787$; MALA: $m = 0.001v + 6.18$, $r^2 = 0.8699$; and SAME: $m = 0.0009v + 19.5$, $r^2 = 0.9536$). ACGL biomass was determined from annual measurements of ACGL fractional cover and density (mass per ground area) in each plot. Fractional cover was measured along an 18.3 m transect in each plot. Density was determined by harvesting and drying ACGL from each plot after measuring plant area.

We accounted for the ANPP of the remaining shrub species at the site (species other than ARCA, MALA, SAME and ACGL) based on cover measurements of all species in each plot (Kimball et al., [25]). We assumed a species' ANPP was proportional to its ground cover; this factor increased overall ANPP an average of 12%. Additionally, our measurements did not include litterfall, which we accounted for based on observations at a nearby, floristically similar shrubland (Vourlitis et al., [45]). We assumed the allocation to biomass increment (mostly stems and other longer-lived tissues) relative to litter production (mostly leaves, flowers and twigs) was similar between sites; this factor increased ANPP by an average of 42%. The resulting shrub ANPP reflects the primary production by perennial woody plants only; it does not include the production by herbaceous plants within shrub plots.

The entire site, including all the grass and shrub plots, burned in the October 2007 Santiago wildfire. The fire had a significant effect on plant species composition for 1–2 years, increasing the abundance of forbs in the grassland and decreasing the abundance of grasses (Goulden et al., in prep). Similarly, the fire increased the abundance of herbaceous plants and ACGL in the shrubland for 3–4 years and decreased the cover of ARCA, MALA and SAME (Kimball et al., [26]). The abundance of grasses and forbs offsets, such that annual grassland ANPP was largely unaffected by the fire and fire recovery. Likewise, ACGL cover offsets ARCA, MALA and SAME cover, which reduced the effect of fire and recovery on coastal sage ANPP.

Climate data

Loma Ridge climate was characterized using several data sources, including daily and annual precipitation and daily potential evapotranspiration. The long-term distribution of annual precipitation was based on a composite of nearby rain gauges (Tustin Irvine Ranch COOP, Santa Ana Fire Station COOP) and the Loma Ridge site rain gauges, resulting in an 83-year record (1929–2012, with the water year defined September through August). All data sources were adjusted to the Loma Ridge observations by linear regression based on overlapping periods. Distributions of daily storm depth and inter-storm duration were estimated from a 104-year record of daily precipitation totals (1906–2010, Santa Ana Fire Station COOP). Lastly, energy availability for evapotranspiration was estimated as daily reference evapotranspiration (ET_0) estimated over a nearby well-watered grassland (CIMIS Irvine, Station 075, 1987–2012). This estimate uses a modified Penman approach.

ANPP Model

Above-ground net primary productivity is modelled by linking plant carbon fluxes to the soil water balance. We assume photosynthesis, respiration, and mortality are entirely dependent on root zone soil moisture (s). Therefore, s is effectively treated as an integrated indicator of the effects of all growth and stress factors (i.e. water, temperature, and nutrient supply). Although each of these factors contributes to ANPP, nutrient supply rates and temperature are closely related to s in dryland ecosystems.

Soil water balance

The soil water balance is defined at the daily scale for a flat vegetated patch overlying a vertically homogeneous soil column with porosity n ($m^3\ m^{-3}$) and active root zone depth z_r (mm),

$$nz_r \frac{ds}{dt} = P_e - E - T - L. \quad (1)$$

Water entering the soil column is denoted the effective precipitation (P_e), or precipitation minus canopy interception and surface runoff. The modelled soil moisture losses are bare soil evaporation (E), transpiration (T) and leakage below the soil column [L; all in units of (mm day^{-1})]. Each of these water fluxes depends on s, and we follow common parameterizations described in the succeeding text (Laio et al., [27]). The model is forced with synthetically generated daily precipitation time series (described in the Section on Meteorological Forcing) and integrated numerically.

Precipitation is assumed to infiltrate instantaneously at the beginning of each wet day. Canopy interception is first subtracted from the total storm depth [h (mm)] and is defined as the product of the vegetated ground fraction (v; Equation) and a parameter describing the water storage capacity of the canopy, c_{max} (mm). Only saturation-excess runoff is considered, which is modelled as the depth of precipitation in excess of the soil storage capacity at the time of the event. With these assumptions, P_e is

$$P_e = \min[h - \min(h, c_{max}v), nz_r(1 - s)]. \tag{2}$$

Evaporation and transpiration are defined as (e.g. Montaldo et al., [32]),

$$E + T = E_p[k_s(1 - v)\beta_s + k_v v\beta_v], \tag{3}$$

where E_p (mm day^{-1}) is the climate-derived potential evapotranspiration, k_s and k_v are dimensionless coefficients that represent physical limits to actual evapotranspiration due to local soil or vegetation conditions, and β_s and β_v represent the reduction in E or T resulting from soil moisture deficit. We assume the β_i's follow piecewise linear functions,

$$\beta_s = \begin{cases} 0 & s \le s_h \\ \dfrac{s - s_h}{s_{fc} - s_h} s_h < s \le s_{fc}, \\ 1 & s > s_{fc} \end{cases} \tag{4a}$$

and

$$\beta_v = \begin{cases} 0 & s \le s_w \\ \dfrac{s - s_w}{s^* - s_w} & s_w < s \le s^* \\ 1 & s > s^* \end{cases} \tag{4b}$$

where s_h(-) is the hygroscopic point, s_{fc} is the field capacity, s_w is the permanent wilting point, and s^* is the incipient stress point.

Total ET is partitioned between E and T, assuming available energy is extinguished exponentially with leaf area. Therefore, the ground fraction contributing to T is

$$v = 1 - \exp(-kL_a), \tag{5}$$

where k (m^{-2} m^2) is the light extinction coefficient and L_a (m^2 m^{-2}) is the leaf area index. L_a is assumed to scale linearly with above-ground biomass, according to the specific leaf area, (m^2 leaf g C^{-1}), assumed constant. It follows that the ground fraction contributing to E is (1 − v).

Lastly, leakage below the root zone is assumed to depend on s similar to the unsaturated hydraulic conductivity,

$$L = K_s \cdot \frac{\exp[\gamma(s - s_{fc})] - 1}{\exp[\gamma(1 - s_{fc})] - 1}, \tag{6}$$

where K_s (mm day^{-1}) is the saturated hydraulic conductivity, c = 2b + 3 represents the decay of conductivity with saturation, where b is the soil pore size distribution index, and γ = 2b + 4.

Vegetation carbon balance

The vegetation carbon balance, including photosynthesis, respiration and water stress-induced mortality, generally follows SVM3 (Montaldo et al., [32] ; see also Istanbulluoglu et al., [19] and references), a relatively simple model shown to perform well in their evaluation of several dynamic vegetation models. The only difference between our model and SVM3 is that we do not explicitly include temperature effects.

The above-ground vegetation carbon balance is

$$\frac{dC_a}{dt} = f_a \cdot NPP - S = f_a\left(A - R_g - R_m\right) - S, \tag{7}$$

where C_a (g C m^{-2}) is the above-ground plant carbon pool, f_a(-) is the fraction of NPP allocated to above-ground growth, and the carbon fluxes are gross photosynthesis (A), growth and maintenance respiration (R_g and R_m), and senescence [S; all in units of (g C m^{-2} day^{-1})].

Photosynthesis is linked to the water balance through the coupled stomatal transport of CO_2 and H_2O. We model A in a fashion similar to T, as a piecewise linear function of s,

$$A = p_{\max}\beta_v v, \tag{8}$$

where p_{max} (g C m^{-2} day^{-1}) is the maximum daily scale photosynthesis rate for a fully vegetated surface and β_v is given by Equation. p_{max} can be interpreted as a constant parameter integrating the light, temperature, and vapour pressure deficit functions in Montaldo et al., ([32]).

Respiration is separated into two components, corresponding to the energy requirements for growth of new plant tissue and maintenance of existing live tissue. R_g is the rate of incoming photosynthate used for new growth, assumed as a constant fraction, k_g, of A. R_m is the rate of incoming photosynthate used to maintain existing tissue, assumed as a constant fraction, k_m, of C_a. These assumptions give the following expression for NPP (Thornley [49]):

$$NPP = y_g A - k_m C_a \tag{9}$$

here $y_g = 1 - k_g$(-) is the growth yield parameter and k_m (day^{-1}) is a biomass-specific maintenance respiration rate.

For drought-deciduous species, such as the grasses and shrubs found at Loma Ridge, senescence is driven by the simultaneous accumulation of water deficit and temperature stresses at the beginning of the summer. We model the role of soil moisture in this process as (Collins and Bras, [9]),

$$S = m(1 - \beta_v)^q C_a, \tag{10}$$

where m (day^{-1}) is the maximum biomass-specific mortality rate and the exponent q represents nonlinearity in the water stress response.

Combining Equations –, the above-ground vegetation carbon balance is,

$$\frac{dC_a}{dt} = f_a y_g p_{max} \beta_v v - [k_m + m(1-\beta_v)^q] C_a \tag{11}$$

where km'=fakm and the effect of soil moisture is evident in the balance of growth and senescence terms. To be consistent with the experimental methodology, modelled grass ANPP is defined as the peak C_a simulated in each year and modelled shrub ANPP is defined as the cumulative sum of NPP and R_m simulated in each year. We assume dry matter production is approximately 0.5 g DM g^{-1} CO_2 (Scholes and Walker, [46]).

Meteorological forcing

The model is forced with synthetic precipitation and ET_0 time series based on long-term statistics. For precipitation, we use a Monte Carlo approach. Simulations for each soil and vegetation parameter set are forced by a 10 000-year time series of rainfall generated as follows. Each year is split into two seasons: a wet winter and a dry summer (Figure [NaN]). The wet season length is denoted T_w, and the dry season length is 365 − T_w. For each wet season, a total precipitation volume, P_a (mm), is sampled from a uniform distribution between 0 and 800 mm, while each dry season is assumed to produce zero rainfall. Within each wet season, a series of rain events is then sampled. We assume storm depths, h, and inter-storm durations, t_s, are independent and exponentially distributed with mean storm depth, α (mm), and mean inter-storm duration, λ^{-1} (day). At Loma Ridge, α and λ vary with P_a such that wetter years are characterized by increased frequency of storms and increased storm intensity (Figure [NaN]). This behaviour is fit by the following relations:

$$a = m_0 \sqrt{P_a}, \tag{12a}$$

and

$$\lambda = (m_0 T_w)^{-1} \sqrt{P_a}, \tag{12b}$$

where m_0 ($mm^{-1/2}$) is a parameter that controls the contribution of α and λ to P_a. m_0 is estimated as 0.65 for Loma Ridge. Using this sampling scheme, the statistics of modelled ANPP and soil water fluxes reflect variability in the timing and intensity of rain events within each wet season and not the distribution of annual precipitation.

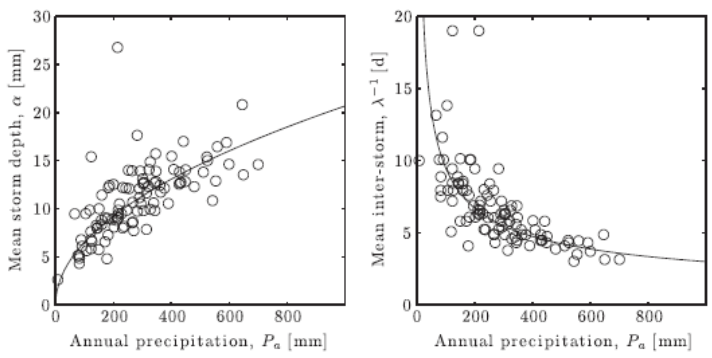

Figure 3. Variability of rainfall model statistics with annual precipitation. The open symbols represent estimates from the long-term daily rainfall record, and the lines correspond to Equations (12a) and (12b) with $m_0 = 0.65$ and $T_w = 145$ days.

The seasonal cycle of E_p is assumed to follow the observed long-term average for each day. A sinusoidal curve is fit to the time series of daily averages,

$$E_p(t) = \overline{E_p} - \Delta E_p \sin(2\pi\omega t), \tag{13}$$

where $\overline{Ep}$=3.45 (mm day^{-1}) is the average daily E_p for all days, ΔE_p = 2.0 (mm day^{-1}) is the amplitude of the seasonal cycle, and ω^{-1} = 365 (day) is the period. t = 0 corresponds to October 1.

Model calibration

The model was parameterized using typical values found in the literature, as summarized in Tables [NaN] and [NaN] , and by calibrating the photosynthesis and stress-induced turnover parameters, p_{max} and m. The model was calibrated to measurements of 15-cm volumetric water content and surface CO_2 and H_2O fluxes measured by eddy covariance. The calibration methodology and results are presented and discussed in the Supporting Information.

Table 1. Soil hydraulic and climate parameters estimated for Loma Ridge.

Parameter[a]		**Units**	**Value**
Porosity	n		0.43
Hygroscopic point	s_h		0.14
Field capacity	s_{fc}		0.56
Pore size distribution index	b		4.39
Saturated hydraulic conductivity	K_s	cm day^{-1}	80
Bare soil evaporation efficiency[b]	k_s		0.5

[a] Soil properties and soil moisture thresholds are those reported by Laio et al. (2012) for sandy loam.
[b] Surface evaporation efficiency is calibrated to observed soil moisture time series and is similar to those reported by Istanbulluoglu et al. (1955).

Table 2. Vegetation parameters estimated for Loma Ridge.

Parameter	**Units**	**Grass**	**Shrub**	**Reference**	
Above-ground allocation fraction	f_a		0.77	0.57	Arora and Boer (2005); Harpole et al. (2007)
Maximum photosynthesis rate	p_{max}	g C m^{-2} days^{-1}	25	20	Calibrated
Biomass yield	y_g		0.75	0.75	Dewar (1996); Istanbulluoglu et al. (19)
Maintenance respiration coefficient	k_m		0.01	0.01	Dewar (1996)
Biomass-specific mortality rate	m	day^{-1}	0.02	0.02	Calibrated
Specific leaf area	SLA	m^2 leaf g C^{-1}	0.01	0.01	Montaldo et al. (33); Istanbulluoglu et al. (19)
Wilting point	s_w		0.18	0.18	Laio et al. (27)
Incipient stress point	s^*		0.46	0.30	Laio et al. (28); Montaldo et al. (33)
Water stress exponent	q		3	3	Laio et al. (23)
Transpiration efficiency	k_v		1	1	Istanbulluoglu et al. (17)

Root depth	z_r	cm	30	125	Hellmers et al. (1955); Holmes and Rice (1996); Schenk and Jackson (2002)
Growing season start date	t_0		45	1	

Results and Discussion

Observed ANPP-P_a responses

The annual grass and drought-deciduous shrub PFTs at Loma Ridge exhibit distinct ANPP-P_a responses (Figure [NaN]). Grass ANPP increases rapidly with increasing P_a for P_a < 240 mm and saturates at a constant value for P_a > 240 mm. Interestingly, this transition point corresponds roughly to the long-term median P_a. Shrub ANPP also increases with P_a, but at a lower, nearly constant rate across all values of P_a. Grasses and shrubs achieve a similar range of ANPP with a maximum of approximately 600 g DM m^{-2} $year^{-1}$ (DM, dry matter). Grass ANPP exceeds shrub ANPP for intermediate P_a (i.e. 200 < P_a <500 mm), whereas ANPP is similar for grasses and shrubs in dry and wet years outside this range.

The ANPP-P_a relations were quantified by regression, with linear and logistic models, and by the ANPP model. The logistic model is defined as

$$ANPP = a_{max}\left\{1 + \left[\frac{1-f}{f}\right]\exp\left[-r\left(P_a - P_f\right)\right]\right\}^{-1}, \quad (14)$$

where a_{max} (g DM m^{-2}) is the saturating value of ANPP, r (mm^{-1}) is a biomass-specific rainfall use efficiency, and f(-) is the fraction of a_{max} at P_f. Both grass and shrub ANPP sensitivity to P_a are best described by the logistic model, as supported by their respective r^2 values (Table [NaN]). Grass ANPP clearly responds to P_a in a logistic fashion, while the logistic model fit for shrubs is nearly linear (Figure [NaN] , Table [NaN]).

Table 3. Linear and logistic model fits to Loma Ridge above-ground net primary productivity (ANPP) data.

Community	**Model**		**r^2**
Grass	Linear	$ANPP = 0.785P_a + 170$	0.46
	Logistic	$ANPP = 547\{1 + 9\exp[-0.025(P_a - 66)]\}^{-1}$	0.83
Shrub	Linear	$ANPP = 0.855P_a - 9.5$	0.79
	Logistic	$ANPP = 821\{1 + 9\exp[-0.005(P_a - 23)]\}^{-1}$	0.81

Above-ground net primary productivity model results are consistent with observations and the logistic model fit (Figure [NaN]). However, compared to the linear and logistic fits, the ANPP model suggests a stronger saturation of shrub ANPP for P_a > 500 mm. Performance of the ANPP model is evaluated in the attached Supporting Information. In the next section, the ANPP model results are explored further, particularly with respect to the correspondence between ANPP and the soil water balance.

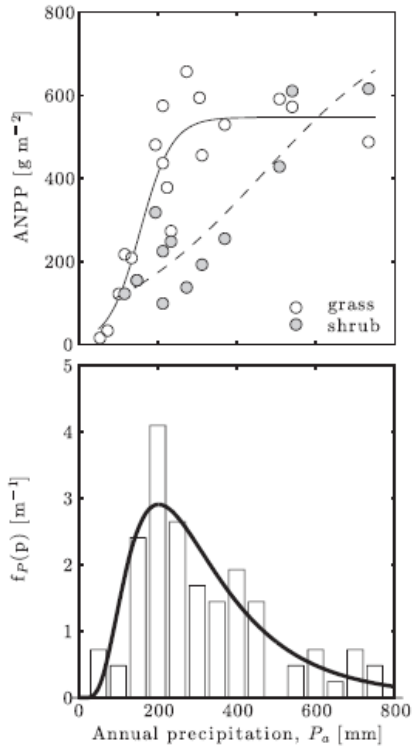

Figure 4. Observed ANPP-P_a relation for Loma Ridge grasses (open symbols, solid line) and shrubs (closed symbols, dashed line). The data are fit with a logistic model (Equation (14)). The long-term P_a distribution is shown in the bottom panel for comparison. ANPP, above-ground net primary productivity; P_a, annual precipitation.

Soil water balance controls on ANPP-P_a responses

The coupled ANPP and soil water balance model results provide a mechanistic interpretation of the observed ANPP-P_a relations. We identify three regimes that highlight the importance of interaction between ecological and hydrological processes in the ANPP response to P_a.

Precipitation compensation point

A minimum precipitation volume, P_{min}, is required to support non-zero productivity. This value was previously defined as 'ineffective precipitation' or the 'zero-yield intercept' (Noy-Meir, [34]). Modelling results suggest grasses and shrubs exhibit a similar P_{min}, which is approximately 100 mm (Figure [NaN]), and P_{min} is controlled by the temporal separation between the wet season and the growing season. Below P_{min}, the soil water balance is entirely partitioned to bare soil evaporation (Figure [NaN]). This non-productive loss is likely concentrated during the initial rainy period, when canopy cover and transpirational demand are low and bare soil and interception evaporation dominates total ET (Eastham et al., [12]). P_a must therefore exceed the early season evaporation demand to support non-zero productivity.

Constant rain-use efficiency

In the second regime, ANPP scales linearly with P_a. Here, transpiration represents an important fraction of the water balance, while evaporation remains constant, and ANPP is truly 'water-limited' (Figures [NaN] and [NaN]). The width of this regime is different for grasses and shrubs. Grass ANPP varies linearly between P_{min} = 100 mm and P_{max} = 260 mm, where grass ANPP saturation is very well-defined above P_{max}. Shrub ANPP observations suggest a nearly linear increase across the entire range of observations, up to at least 600 mm. Alternatively, model results suggest shrub ANPP may saturate at approximately 500 mm of rainfall. In either case, this regime of the shrub ANPP-P_a curve is characterized by a lower slope and a wider P_a range than that for grasses.

The slope of the ANPP-P_a curve in this regime is equivalent to the maximum rain-use efficiency (RUE) (LeHouerou, [30]). Loma Ridge RUEs estimated from the logistic model fits are 2.1 g DM m^{-2} mm^{-1} H_2O for grasses and 0.9 g DM m^{-2} mm^{-1} H_2O for shrubs. These values are consistent with those previously reported for water-limited ecosystems, which typically range between 0.5 and 2 g DM m^{-2} mm^{-1} H_2O (Noy-Meir, [34] ; LeHouerou, [30] ; Sala et al., [39]). Loma Ridge RUE also falls within the range expected for C_3 grasses and shrubs. Photosynthetic water use efficiency of C_3 grasses typically ranges between 2 and 5 mmol CO_2 mol^{-1} H_2O, while that of C_3 shrubs may be as high as 11 (Lambers et al., [29]). Assuming growth and maintenance respiration accounts for approximately half of carbon assimilated by photosynthesis (Cannell and Thornley, [4]) and dry matter production is approximately 0.5 g DM g^{-1} CO_2 (Scholes and Walker, [40]), then 1.2 < RUE < 3 for grasses and 1.2 < RUE < 6.6 for shrubs.

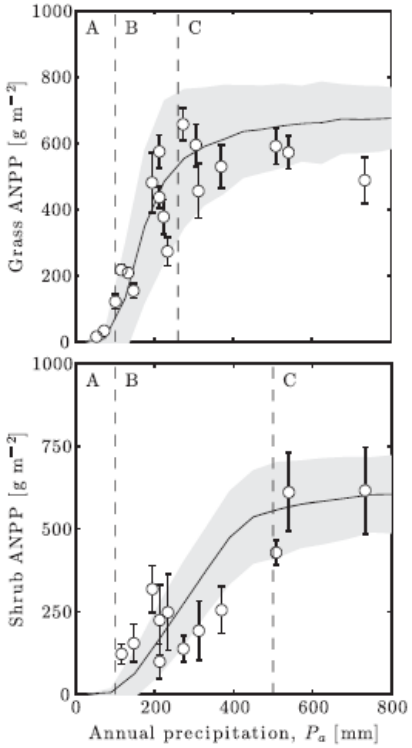

Figure 5. Modelled ANPP-P_a relation for Loma Ridge grasses (top) and shrubs (bottom). The dashed line corresponds to the mean over 10 000 precipitation realizations, and the grey region corresponds to two standard deviations around this mean. Observations are indicated by open symbols (μ ± SE, n = 8). The three ANPP regimes are marked by the letters: A = precipitation compensation point, B = constant rain-use efficiency and C = ANPP saturation. ANPP, above-ground net primary productivity; P_a, annual precipitation.

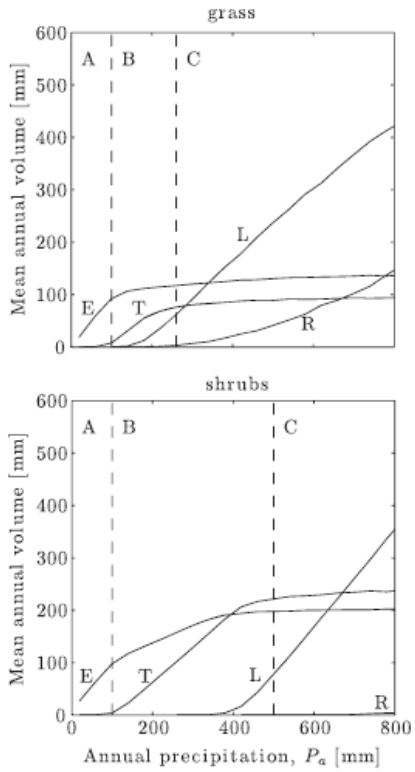

Figure 6. Modeled mean annual water balance components as a function of annual precipitation for modeled grasses (top) and shrubs (bottom). E: evaporation; T: transpiration; L: leakage; R: runoff. Model forcing is the same as that in Figure 5.

ANPP saturation

Finally, grass and possibly shrub ANPP saturate at high P_a. The modelled water balance suggests that the saturation point, P_{max}, is related to progressively increasing non-productive leakage and runoff losses. P_{max} is associated with the point where leakage plus runoff is approximately 15% of the water balance for both PFTs. The fraction of the modelled water balance partitioned to non-productive leakage and runoff losses increases with P_a for both PFTs (Figure [NaN]). Both fluxes are overall higher for grass, which has a smaller root zone depth (Table [NaN]). Because leakage and runoff depend strongly on soil moisture, these fluxes are most important early in the growing season when the soil is more saturated. Similar to early season evaporation in dry years, leakage and runoff represent a fraction of P_a that the ecosystem cannot utilize to support productivity. It is also possible that productivity is limited by other factors such as light or nutrients in wet years.

Evaporation-transpiration partitioning in seasonally dry climates

In addition to the aforementioned interpretation of inter-annual ANPP variability, the model results provide an estimate of the partitioning of total ET into the individual contributions of E and T. Across the precipitation gradient, E is typically greater than T for both grasses and shrubs, with the exception of shrubs in wet years (Figure [NaN]). Under well-watered conditions, the ratio T/ET is approximately 0.40 for grasses and 0.54 for shrubs. These values are consistent with recent estimates from stable isotope and experimental studies that place T/ET between 0.35 and 0.80 (Coenders-Gerrits et al., [25] ; Wang et al., [52]). However, data from seasonally dry climates is notably absent in these estimates.

There is reason to hypothesize T/ET ratios in seasonally dry climates fall at the lower end of the estimated range. Of the studies analysed by Wang et al. ([52]), three have characteristics similar to the Loma Ridge site. In two semi-arid shrublands in the North American monsoon region, T/ET ratios were 42% and 47% (Cavanaugh et al., [7]). In a seasonally dry, semi-arid Eucalypt woodland, T/ET was measured at 53% and 22% in the summer and

winter, respectively (Mitchell et al., [31]). In winter-sown, rain-fed crops in a seasonally dry climate, the T/ET ratio was 50% and 46% for two different row spacings (Eberbach and Pala, [13]). As mentioned in the previous text, low T/ET ratios in these environments may be related to asynchrony of rainfall and productivity (e.g. Eastham et al., [12]), a pattern consistent with our simulations.

Resource use strategies, ANPP-P_a responses and climate

The observed and modelled ANPP-P_a patterns suggest a specific role for ecohydrological mechanisms in inter-annual ANPP variability at Loma Ridge. In dry years, productivity is constrained by asynchrony between the wet and growing seasons and the resulting seasonality of bare soil evaporation. In wet years, productivity is constrained by root zone soil moisture storage and its effect on leakage and runoff. Productivity scales directly with precipitation only in intermediate rainfall years. The relative importance of these controls across a precipitation gradient varies with resource use strategy, as supported by the comparison between Loma Ridge grass and shrub observations. This interaction between resource use strategies, ANPP and climate is now discussed, specifically in relation to root depth, water stress tolerance, and respiration.

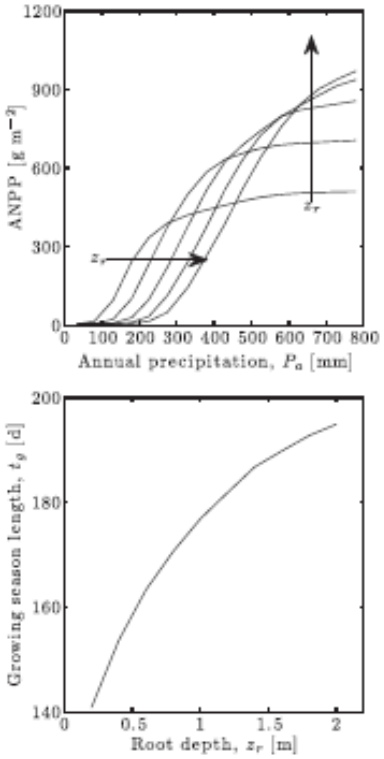

Figure 7. The effect of rooting depth, z_r, on the ANPP-Pa relation: (top) ANPP versus P_a for several values of z_r, ranging between 20 and 180 cm. The arrows point in the direction of increasing z_r. (bottom) Growing season length, t_g, as a function of rooting depth, z_r. Vegetation parameters are those estimated for Loma Ridge annual grassland (Table II). ANPP, above-ground net primary productivity; P_a, annual precipitation.

Root zone depth (z_r) regulates a trade-off between the total volume of plant available water and the carbon cost of below-ground productivity. The shallow grass z_r constrains plant available water and increases non-productive losses, modelled here as leakage and saturation-excess runoff. On the other hand, the deeper shrub z_r is associated with increased moisture storage and access to moisture stored at deeper soil layers, which effectively limits non-productive losses. Because of these effects, z_r controls the main features of the modelled ANPP-P_a response, predicting a trade-off between the precipitation compensation point (P_{min}) and the saturating ANPP (a_{max}), all other parameters being equal (Figure [NaN] a). Water stress limits productivity in dry years, and therefore, P_{min} increases with z_r as the modelled s decreases. The modelled a_{max} also increases with z_r. Measuring

the growing season length as the time to maximum biomass, the model predicts an increased growing season length with z_r (Figure [NaN] b). Deep-rooted plants have access to a larger store of water, allowing a longer period of growth before the wilting point is reached and, therefore, higher a_{max}. Considering variation in z_r alone, the model suggests a lengthened growing season comes at the expense of a higher precipitation requirement for positive productivity. This modelling result provides a physical basis for productivity-resource responses previously hypothesized (Pastor and Bridgham, [35]). However, the cost of deep roots, including increased below-ground allocation and root maintenance respiration, may compromise the ability of shrubs to achieve the predicted increase in a_{max}. Indeed, in wet years, Loma Ridge grasses and shrubs reach a similar maximum ANPP (Figure [NaN]), while shrub gross ecosystem exchange is typically twice that of grasses (Figure S3).

Deep-rooted species may compensate for increased P_{min} through a lower sensitivity to water stress. The point of incipient water stress (s^*) is typically lower for woody species than for herbaceous species (Scholes and Walker, [46] ; Williams and Albertson, [53]), which improves function under chronically low soil moisture levels. Further, because woody plants maintain a coarse root structure between years, they may be better able to adapt the depth of root water uptake and to integrate deep stored moisture with intermittent infiltration at the surface to improve productivity in dry years (Sivandran and Bras, [48]). Our model confirms that increased resilience of productivity under water stress, represented by lower s^*, offsets the increased P_{min} associated with deep roots.

Rain-use efficiency and ecosystem organization

Grasses and shrubs demonstrate different RUE patterns across the precipitation gradient, which the model suggests results from the combined effects of root depth, below-ground allocation, respiration, and water stress on ANPP. The slope of the ANPP-P_a curve in intermediate precipitation years indicates that shrub RUE is approximately half of grass RUE. Therefore, assuming RUE is a good indicator of ecological success, it can be concluded grasses are at an advantage in this ecosystem under typical precipitation conditions. Although shrub RUE is less than grass RUE during most years, shrubs achieve a comparable RUE in dry or wet years (Figure [NaN]). This suggests these unlikely rainfall years may be critical to the maintenance of shrub populations at Loma Ridge. Along the Kalahari transect, another savanna-like ecosystem, the mixed tree–grass ecosystem state was shown to maximize a combined measure of transpiration and water stress across a wider range of P_a than either homogeneous community (Caylor et al., [6]). In addition, the observed relative tree–grass cover in this ecosystem is associated with a soil water balance that simultaneously limits water stress and leakage (Scanlon and Albertson, [41]). The data presented here support these previous conclusions and demonstrate that efficient use of the soil water balance is fundamentally related to the ANPP-P_a curves of the component PFTs. At Loma Ridge, shrubs are sub-optimal under typical rainfall conditions but achieve a competitive RUE during infrequent dry and wet years, whereas grasses appear to exploit the most likely climatic conditions.

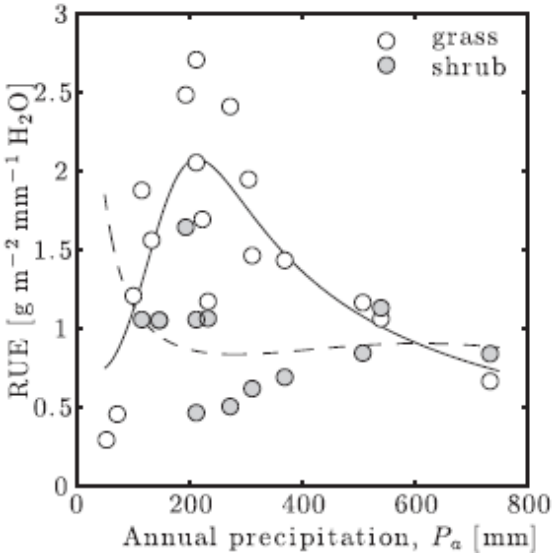

Figure 8. Rain-use efficiency (RUE) estimates for Loma Ridge grasses (open symbols, solid line) and shrubs (closed symbols, dashed line) derived from the logistic models fit to the observed ANPP-P_a relation. ANPP, above-ground net primary productivity; P_a, annual precipitation.

The observed relations between ANPP, RUE and the long-term P_a distribution may indicate an underlying organization between climate, ecosystem resource use efficiency, and biogeography. First, note that grass ANPP saturates and grass RUE are maximum at the observed median P_a (Figures [NaN] and [NaN]). Grass ANPP saturation may be related to the emergence of a biogeochemical constraint to productivity, such as nitrogen supply, under high rainfall conditions (Yahdjian et al., [54]). If grass ANPP saturation at Loma Ridge was indeed the result of a biogeochemical constraint, our results would indicate that these constraints are linked with climate. For example, nutrient supply rates in Loma Ridge grassland may be such that the maximum, nutrient-limited ANPP is achieved under average climate conditions. Therefore, we might expect the saturation point, P_{max}, for similar PFTs to vary with the mean P_a across climates and soil types. Secondly, grass–shrub co-occurrence may be viewed as a mechanism by which ecosystem-scale ANPP and RUE are maximized across a wider range of P_a than either community can achieve in isolation. We hypothesize the presence of shrubs allows for a deeper root depth in high rainfall years beyond that which could be achieved with annual grasses alone. In a mixed ecosystem, the physiological constraint of limited grass root depth is compensated by the addition of deep-rooted shrubs, a viable solution to an optimization problem constrained by PFT traits and availability.

Conclusions

We analysed the ANPP response to annual precipitation in annual grassland and drought-deciduous shrubland in a seasonally dry, semi-arid climate. A multi-year rainfall manipulation experiment revealed a nonlinear, saturating ANPP-P_a response in grassland and a contrasting linear response in shrubland. We applied a simple ANPP model based on the soil water balance to explore the mechanisms by which the land surface response to precipitation modulates inter-annual ANPP variability. Assuming transpiration and soil moisture deficit as the primary controls on ANPP, the coupled ANPP-soil water balance model reproduced the general features of the ANPP-P_a relation in both communities. From a mechanistic viewpoint, the model suggests several ecohydrological factors govern this relation: (1) asynchrony between the wet season and the growing season, which promotes bare soil evaporation; (2) root depth, which controls infiltration rates, soil water storage, root water access and growing season length; and (3) incipient stress point, which controls the resilience of productivity under water stress. Together, these factors suggest that although shrubs are less efficient water users under average precipitation, their increased below-ground allocation and respiration demand are offset by resilience under water stress and a longer growing season, possibly conferring shrubs' competitive advantage in

dry and wet years. Because rain-use efficiency was asymmetric across the experimentally imposed precipitation gradient, inter-annual precipitation variability may be critical to grass–shrub coexistence in this ecosystem.

Acknowledgements

The authors gratefully acknowledge support from the U.S. Department of Energy through grant FG02-05ER64021, the National Science Foundation through grant EAR 0962253, and the Kuwait-MIT Center for Natural Resources and the Environment. We also thank the anonymous reviewers for helpful comments on previous versions of this manuscript.

References

1 *Arora VK, Boer GJ. 2005. A parameterization of leaf phenology for the terrestrial ecosystem component of climate models. Global Change Biology 11 : 39 – 59. DOI: 10.1111/j.1365-2486.2004.00890.x*

2 *Bartolome JW, Barry WJ, Griggs T, Hopkinson P. 2007. Valley grassland. In Terrestrial Vegetation of California, Barbour MG, Keeler-Wolf T, Schoenherr AA (eds). University of California Press : Berkeley, CA ; 367 – 393.*

3 *Briggs JM, Knapp AK. 1995. Interannual variability in primary production in tallgrass prairie: climate, soil moisture, topographic position, and fire as determinants of aboveground biomass. American Journal of Botany 82 : 1024 – 1030.*

4 *Budyko, MI. 1974. Climate and Life. Academic Press Inc. : New York, NY.*

5 *Cannell MGR, Thornley JHM. 2000. Modelling the components of plant respiration: some guiding principles. Annals of Botany 85 : 45 – 54. DOI: 10.1006/anbo.1999.0996*

6 *Caylor KK, Scanlon TM, Rodriguez-Iturbe I. 2009. Ecohydrological optimization of pattern and processes in water-limited ecosystems: a tradeoff-based hypothesis. Water Resources Research 45 : W08407. DOI: 10.1029/2008WR007230.*

7 *Cavanaugh ML, Kurc SA, Scott RL. 2011. Evapotranspiration partitioning in semiarid shrubland ecosystems: a two-site evaluation of soil moisture control on transpiration.* ***Ecohydrology*** *4 : 671 – 681. DOI: 10.1002/eco.157*

8 *Coenders-Gerrits AMJ, van der Ent RJ, Bogaard TA, Wang-Erlandsson L, Hrachowitz M, Savenije HHG. 2014. Nature 506 : E1. DOI: 10.1038/nature12925*

9 *Collins DBG, Bras RL. 2010. Climatic and ecological controls of equilibrium drainage density, relief, and channel concavity in drylands. Water Resources Research 46 : W04508. DOI: 10.1029/2009WR008615*

10 *del Jesus M, Foti R, Rinaldo A, Rodriguez-Iturbe I. 2012. Maximum entropy production, carbon assimilation, and the spatial organization of vegetation in river basins. Proceedings of the National Academy of Sciences of the USA 109 : 20837 – 20841. DOI: 10.1073/pnas.1218636109*

11 *Dewar RC. 1996. The correlation between plant growth and intercepted radiation: an interpretation in terms of optimal plant nitrogen content. Annals of Botany 78 : 125 – 136. DOI: 10.1006/anbo.1996.0104*

12 *Eastham J, Gregory PJ, Williamson DR, Watson GD. 1999. The influence of early sowing of wheat and lupin crops on evapotranspiration and evaporation from the soil surface in a Mediterranean climate. Agricultural Water Management 42 : 205 – 218. DOI: 10.1016/S0378-3774(99)00036-0*

13 *Eberbach P, Pala M. 2005. Crop row spacing and its influence on the partitioning of evapotranspiration by winter-grown wheat in Northern Syria. Plant and Soil 268 : 195 – 208. DOI: 10.1007/s11104-004-0271*

14 *Feng X, Vico G, Porporato A. 2012. On the effects of seasonality on soil water balance and plant growth. Water Resources Research 48 : W05543. DOI: 10.1029/2011WR011263*

15 *Goulden ML, Parker SC, Suding KN, Potts DL, Winston GC, Kimball S. in prep. Global-change manipulations abruptly shift post-fire trajectories of grassland productivity and community composition.*

16 *Harpole WS, Potts DL, Suding KN. 2007. Ecosystem responses to water and nitrogen amendment in a California grassland. Global Change Biology 13 : 2341 – 2348. DOI: 10.1111/j.1365-2486.2007.01447.x*

17 *Hellmers H, Horton JS, Juhren G, O'Keefe J. 1955. Root systems of some chaparral plants in southern California. Ecology 36 : 667 – 678. DOI: 10.2307/1931305*

18 *Holmes TH, Rice KJ. 1996. Patterns of growth and soil-water utilization in some exotic annuals and native perennial bunchgrasses of California. Annals of Botany 78 : 233 – 243. DOI: 10.1006/anbo.1996.0117*

19 Hsu JS, Powell J, Adler PB. 2012. Sensitivity of mean annual primary productivity to precipitation. Global Change Biology 18 : 2246 – 2255. DOI: 10.1111/j.1365-2486.2012.02687.x
20 Huxman TE, Smith MD, Fay PA, Knapp AK, Shaw MR, Loik ME, Smith SD, Tissue DT, Zak JC, Weltzin JF, Pockman WT, Sala OE, Haddad BM, Harte J, Koch GW, Schwinning S, Small EE, Williams DG. 2004. Convergence across biomes to a common rain-use efficiency. Nature 429 : 651 – 654. DOI: 10.1038/nature02561
21 Hwang T, Band L, Hales TC. 2009. Ecosystem processes at the watershed scale: extending optimality theory from plot to catchment. Water Resources Research 45 : W11425. DOI: 10.1029/2009WR007775
22 Istanbulluoglu E, Wang T, Wedin DA. 2012. Evaluation of ecohydrologic model parsimony at local and regional scales in a semiarid grassland ecosystem. **Ecohydrology** 5 : 121 – 142. DOI: 10.1002/eco.211
23 Ivanov VY, Bras RL, Vivoni ER. 2008a. Vegetation-hydrology dynamics in complex terrain of semiarid areas: 1. A mechanistic approach to modeling dynamic feedbacks. Water Resources Research 44 : W03429. DOI: 10.1029/2006WR005588
24 Ivanov VY, Bras RL, Vivoni ER. 2008b. Vegetation-hydrology dynamics in complex terrain of semiarid areas: 2. Energy-water controls of vegetation spatiotemporal dynamics and topographic niches of favorability. Water Resources Research 44 : W03430. DOI: 10.1029/2006WR005595
25 Jin Y, Goulden ML. 2014. Ecological consequences of variation in precipitation: separating short- versus long-term effects using satellite data. Global Ecology and Biogeography 23 : 358 – 370. DOI: 10.1111/geb.12135
26 Kimball S, Goulden ML, Suding KN, Parker S. 2014. Altered water and nitrogen input shifts succession in a Southern California coastal sage community. Ecological Applications 24 : 1390 – 1404. DOI: 10.1890/13-1313.1
27 Laio F, Porporato A, Ridolfi L, Rodriguez-Iturbe I. 2001a. Plants in water-controlled ecosystems: active role in hydrologic processes and response to water stress: II. Probabilistic soil moisture dynamics. Advances in Water Resources 24 : 707 – 723. DOI: 10.1016/S0309-1708(01)00005-7
28 Laio F, Porporato A, Fernandez-Illescas CP, Rodriguez-Iturbe I. 2001b. Plants in water-controlled ecosystems: active role in hydrologic processes and response to water stress: IV. Discussion of real cases. Advances in Water Resources 24 : 745 – 762. DOI: 10.1016/S0309-1708(01)00007-0
29 Lambers H, Chapin III FS, Pons TL. 2008. Plant Physiological Ecology, 2nd ed. Springer, New York, NY.
30 LeHouerou HN. 1984. Rain use efficiency: a unifying concept in arid-land ecology. Journal of Arid Environments 7 : 213 – 247.
31 Mitchell PJ, Veneklaas E, Lambers H, Burgess SSO. 2009. Partitioning of evapotranspiration in a semi-arid eucalypt woodland in south-western Australia. Agricultural and Forest Meteorology 149 : 25 – 37. DOI: 10.1016/j.agrformet.2008.07.008
32 Montaldo N, Rondena R, Albertson JD, Mancini M. 2005. Parsimonious modeling of vegetation dynamics for ecohydrologic studies of water-limited ecosystems. Water Resources Research 41 : W10416. DOI: 10.1029/2005WR004094
33 Montaldo N, Albertson JD, Mancini M. 2008. Vegetation dynamics and soil water balance in a water-limited Mediterranean ecosystem on Sardinia, Italy. Hydrology and Earth System Sciences 12 : 1257 – 1271. DOI: 10.5194/hess-12-1257-2008
34 Noy-Meir I. 1973. Desert ecosystems: environment and producers. Annual Review of Ecology and Systematics 4 : 25 – 51. DOI: 10.1146/annurev.es.04.110173.000325
35 Pastor J, Bridgham SD. 1999. Nutrient efficiency along nutrient availability gradients. Oecologia, 118 : 50 – 58. DOI: 10.1007/s004420050702
36 Reynolds JF, Smith DMS, Lambin EF, Turner II BL, Mortimore M, Batterbury SPJ, Downing TE, Dowlatabadi H, Fernandez RJ, Herrick JE, Huber-Sannwald E, Jiang H, Leemans R, Lynam T, Maestre, FT, Ayarza M, Walker B. 2007. Global desertification: building a science for dryland development. Science 316 : 847 – 851. DOI: 10.1126/science.1131634
37 Rietkerk M, Dekker SC, de Ruiter PC, van de Koppel J. 2004. Self-organized patchiness and catastrophic shifts in ecosystems. Science 305 : 1926 – 1929. DOI: 10.1126/science.1101867

38 Rundel PW. 2007. Sage scrub. In Terrestrial Vegetation of California, Barbour MG, Keeler-Wolf T, Schoenherr AA (eds). University of California Press : Berkeley, CA ; 208 – 228.
39 Sala OE, Parton WJ, Joyce LA, Lauenroth WK. 1988. Primary production of the central grassland region of the United States. Ecology 69 : 40 – 45. DOI: 10.2307/1943158.
40 Sala OE, Gherardi LA, Reichmann L, Jobbagy E, Peters D. 2012. Legacies of precipitation fluctuations on primary production: theory and data synthesis. Philosophical Transactions of the Royal Society B 367 : 3135 – 3144. DOI: 10.1098/rstb.2011.0347
41 Scanlon TM, Albertson JD. 2003. Inferred controls on tree/grass composition in a savanna ecosystem: combining 16-year normalized difference vegetation index data with a dynamic soil moisture model. Water Resources Research 39 : 1224. DOI: 10.1029/2002WR001881
42 Schenk HJ, Jackson RB. 2002. Rooting depths, lateral root spreads and below-ground/above-ground allometries of plants in water-limited ecosystems. The Journal of Ecology 90 : 480 – 494. DOI: 10.1046/j.0022-0477.2002.00683.x
43 Schlesinger WH, Reynolds JF, Cunningham GL, Huenneke LF, Jarrell WM, Virginia RA, Whitford WG. 1990. Biological feedbacks in global desertification. Science 247 : 1043 – 1048. DOI: 10.1126/science.247.4946.1043.
44 Schneider S, Semenov S, Patwardhan A, Burton I, Magadza C, Oppenheimer M, Pittock A, Rahman A, Smith J, Suarez A, Yamin F. 2007, Assessing key vulnerabilities and the risk from climate change, in climate change 2007: impacts, adaptation and vulnerability. In Fourth Assessment Report of the Intergovernmental Panel on Climate Change, Parry M, Canziani O, Palutikof J, van der Linden P, Hanson C (eds). Cambridge University Press, Cambridge.
45 Scholes RJ, Archer SR. 1997. Tree-grass interactions in savannas. Annual Review of Ecology and Systematics 28 : 517 – 544. DOI: 10.1146/annurev.ecolsys.28.1.517
46 Scholes RJ, Walker BH. 1993. An African Savanna: Synthesis of the Nylsvley Study. Cambridge University Press, Cambridge.
47 Schwinning S, Ehleringer JR. 2001. Water use trade-offs and optimal adaptations to pulse-driven arid ecosystems. Journal of Ecology 89 : 464 – 480. DOI: 10.1046/j.1365-2745.2001.00576.x
48 Sivandran G, Bras RL. 2013. Dynamic root distributions in ecohydrological modeling: a case study at Walnut Gulch Experimental Watershed. Water Resources Research 49 : 3292 – 3305. DOI: 10.1002/wrcr.20245
49 Thornley JHM. 1970. Respiration, growth and maintenance in plants. Nature 227 : 304 – 305. DOI: 10.1038/227304b0
50 Viola F, Daly E, Vico G, Cannarozzo M, Porporato A. 2008. Transient soil-moisture dynamics and climate change in Mediterranean ecosystems. Water Resources Research 44 : W11412. DOI: 10.1029/2007WR006371
51 Vourlitis GL, Pasquini DC, Mustard R. 2009. Effects of dry-season N input on the productivity and N storage of Mediterranean-type shrublands. Ecosystems 12 : 473 – 488. DOI: 10.1007/s10021-009-9236-6
52 Wang L, Good SP, Caylor KK. 2014. Global synthesis of vegetation control on evapotranspiration partitioning. Geophysical Research Letters 41 : 6753 – 6757. DOI: 10.1002/2014GL061439
53 Williams CA, Albertson JD. 2004. Soil moisture controls on canopy-scale water and carbon fluxes in an African savanna. Water Resources Research 40 : W09302. DOI: 10.1029/2004WR003208
54 Yahdjian L, Gherardi L, Sala OE. 2011. Nitrogen limitation in arid-subhumid ecosystems: a meta-analysis of fertilization studies. Journal of Arid Environments 75 : 675 – 680. DOI: 10.1016/j.jaridenv.2011.03.003
55 van Wijk MT, Rodriguez-Iturbe I. 2002. Tree-grass competition in space and time: insights from a simple cellular automata model based on ecohydrological dynamics. Water Resources Research 38 : 1179. DOI: 10.1029/2001WR000768

Supporting Information

Ecohydrological controls on grass and shrub above-ground net primary productivity in a seasonally-dry climate

Supplemental Information: Model validation and flux data.

Data

Model performance is assessed by comparison to observed soil moisture and surface CO_2 and H_2O fluxes during the 2007-2008 growing season (Figures S1 and S2 below). The model is forced by precipitation and potential evapotranspiration as described in the text. Soil and vegetation parameters were chosen from typical published values or calibrated to match observations (see Tables 2 and 3 in the text). Observations are as follows:

Soil moisture. Volumetric water content was recorded at 2–4 week intervals by time domain reflectometry using 15 cm waveguides (MiniTrase, ICT International). Probes were installed vertically at the soil surface, providing an estimate of average water content over the upper 15 cm of soil.

Gross primary productivity (GPP) and evapotranspiration (ET). Surface CO_2 and H_2O fluxes were measured by eddy covariance (see Goulden et al., 2012 for details on experimental set-up and data processing).

Discussion

The model provides a reasonable representation of the seasonal water and carbon dynamics for both grasses and shrubs at Loma Ridge. There are a number of caveats, however, that limit interpretation of the modeling results and are noted below.

First, note that the model under-predicts the observed cumulative water vapor flux in grassland (Figure S1b). The model predicts 173 mm evapotranspiration, whereas the estimate from the eddy covariance data is 300±60 mm. Precipitation was 223 mm between October 2007 and September 2008. Therefore, the model predicts an ET/P ratio of approximately 0.78 and the observations provide an estimate of 1.35. The modeled ET/P ratio is on the low end, but consistent with modeled and observed values in other seasonally-dry, semi-arid ecosystems (Potter et al., 2005; Feng et al., 2012; Gentine et al., 2012). On the other hand, the observations suggest a water vapor source in addition to the current year precipitation. The water source may be stored water from previous years, transpired by deeper rooted vegetation, or re-evaporation of morning dew, which is frequently observed at the site. However, additional information is needed to distinguish between these 2 hypotheses.

Modeled GPP, ET, and soil moisture match the observations well in the shrub plots (Figure S2). Although the model predicts total GPP at the end of the growing season, the seasonal dynamics of carbon accumulation are delayed in the model relative to the observations. This is likely due to a storage effect, enhanced by the choice of a large z_r for the shrub simulations, which effectively slows the model dynamics. This effect can also be identified in the modeled soil moisture trajectory, which exhibits less variability than the 15 cm surface measurements. Such inconsistencies in the time-scale of soil moisture depletion is a well-known artifact in the lumped root zone model employed here (e.g. Guswa et al., 2004); however, it does not seem to affect the prediction at the annual scale.

The effect of rooting depth on model results provides some additional insight into the ET discrepancy in the grass simulations. The ET/P ratio increases with rooting depth. Both observed and modeled shrub ET resulted in estimated ET/P ratios of 1.04 and 1.02, respectively, consistent with such semi-arid ecosystems. Modeled ET in grass does respond positively to increased z_r, which increases soil moisture storage and the supply of water to ET. However, water stress increases and productivity decreases as well (data not shown). Therefore, the model

assumptions contain a trade-off between accuracy of ET and ANPP measurements; and the parameters chosen here effectively balance that trade-off in the results.

References

Feng, X., G. Vico, and A. Porporato. (2012). On the effects of seasonality on soil water balance and plant growth. *Water Resources Research*, Vol. 48, W05543, doi:10.1029/2011WR011263.

Gentine, P., P. D'Odorico, B.R. Litner, G. Sivandran, and G. Salvucci. (2012). Interdependence of climate, soil, and vegetation as constrained by the Budyko curve. *Geophysical Research Letters*, Vol. 39, L19404, doi:10.1029/2012GL053492.

Goulden, M.L., R.G. Anderson, R.C. Bales, A.E. Kelly, M. Meadows, and G.C. Winston. (2012). Evapotranspiration along an elevation gradient in California's Sierra Nevada. *Journal of Geophysical Research Biogeosciences*, Vol. 117, G03028, doi:10.1029/2012JG002027.

Guswa, A.J., M.A. Celia, and I. Rodriguez-Iturbe. (2004). Effect of vertical resolution on predictions of transpiration in water-limited ecosystems. *Advances in Water Resources*, 27, 467-480.

Potter, N.J., L. Zhang, P.C.D. Milly, T.A. McMahon, and A.J. Jakeman. (2005). Effects of rainfall seasonality and soil moisture capacity on mean annual water balance for Australian catchments. *Water Resources Research*, Vol. 41, W06007, doi:10.1029/2004WR003697.

Figures

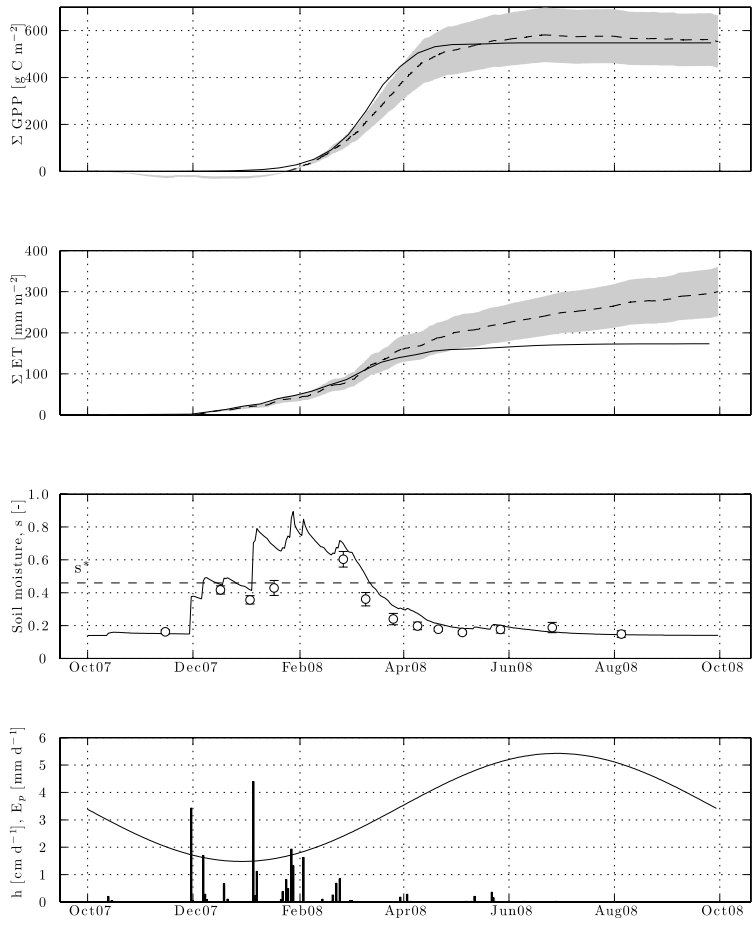

Figure S1. Observed and modeled water balance and carbon dynamics for Loma Ridge grassland during the 2007-2008 growing season: (a) gross primary productivity; (b) evapotranspiration; (c) soil moisture; and (d) daily precipitation and potential evapotranspiration. The gray regions in panels (a) and (b) represent +/- 20% of the cumulative sums of GPP and ET.

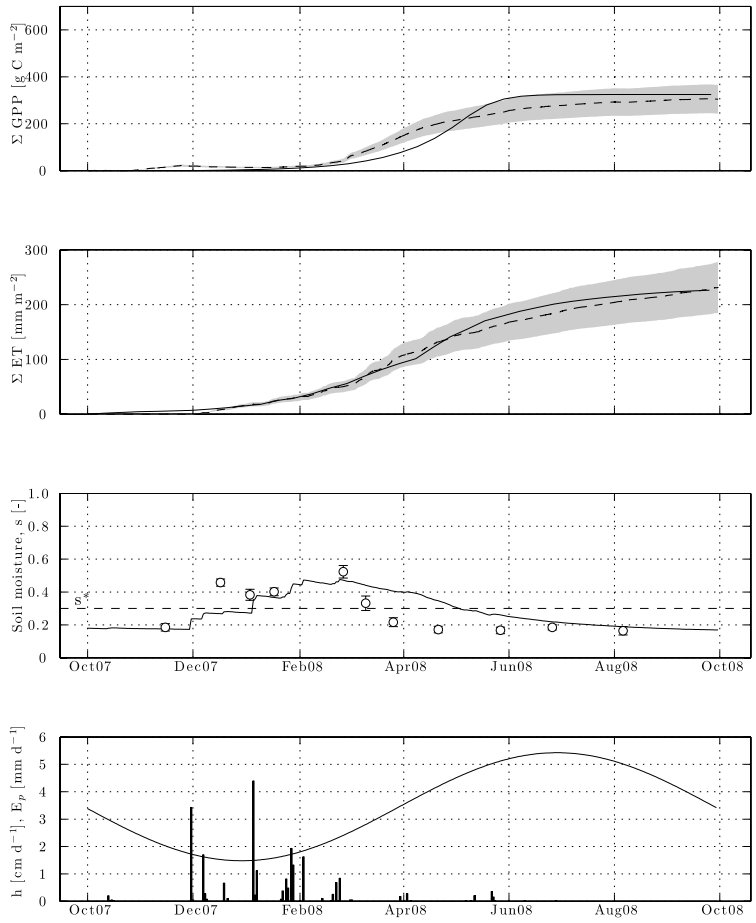

Figure S2. Observed and modeled water balance and carbon dynamics for Loma Ridge shrubland during the 2007-2008 growing season: (a) gross primary productivity; (b) evapotranspiration; (c) soil moisture; and (d) daily precipitation and potential evapotranspiration. The gray regions in panels (a) and (b) represent +/- 20% of the cumulative sums of GPP and ET.

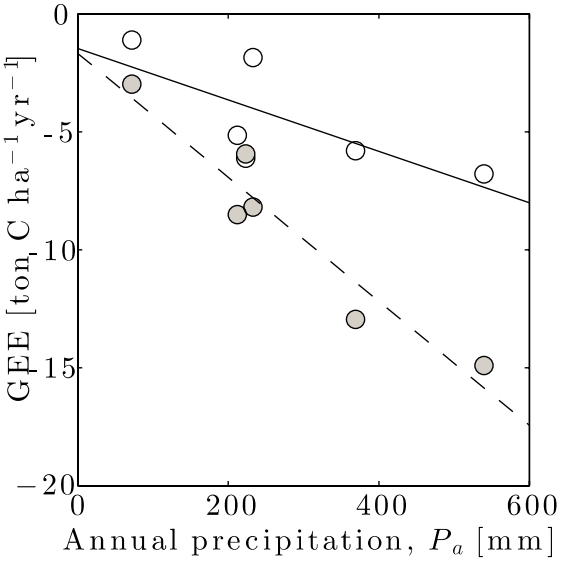

Figure S3. Gross ecosystem exchange (GEE) for Loma Ridge grasses (open symbols, solid line) and shrubs (closed symbols, dashed line) estimated from eddy covariance observations. Linear regressions are: GEE=-0.0263*P_a-1.665 (r^2=0.917) for shrubs and GEE=-0.0109*P_a-1.467 (r^2=0.538) for grasses.